Coacervate Formation and Structural Changes during Dilution Process of Non-Sulfate Shampoos: Study Using an Anionic Surfactant Sodium Lauroyl Aspartate Model Formulation

Hikari Kamo¹, Toshihiro Mori^{1,2} and Katsunori Yoshida*,¹
¹Skin Science Lab, School of Pharmacy, Kitasato University, Tokyo, Japan
²Skincare Lab, Mandom Corporation, Osaka, Japan

Shampoos contain key ingredients such as cationic polymers, anionic surfactants, and amphoteric surfactants. These components are known to undergo liquid-liquid phase separation, called coacervation, at specific relative concentrations during dilution with water when used. Recently, non-sulfate shampoos have become increasingly popular, but there are insufficient research reports on coacervation in this system. In previous work, the authors investigated coacervation and the properties of the coacervates generated during dilution using commercial non-sulfate shampoos. However, due to the lack of detailed information on the ingredients in commercial products, it was difficult to manipulate the factors influencing coacervation. Therefore, model shampoos were developed using cationic polymers, anionic/amphoteric surfactants, and salts with known compositions. In this study, the model shampoos were analyzed using turbidity, dynamic light scattering, ζ-potential, rheological measurements, and microscopy to observe coacervation and the structure of the coacervates formed during dilution. The results showed that the model shampoos underwent coacervation during the dilution process, and the coacervates exhibited more elastic properties at lower relative concentrations. Additionally, their structure transitioned from a hexagonal liquid crystalline to a lamellar one. These findings suggest that the dilution process in non-sulfate shampoos leads to distinct structural changes in the coacervates, offering insights into the formulation design for improved product performance.

Key words: coacervation, coacervate, shampoo, non-sulfate, dilution, mixed micelle, anionic surfactant, amphoteric surfactant, polycation, structural change, hexagonal phase, lamellar phase, turbidity, dynamic light scattering (DLS), ζ -potential, fluorescence, rheology, polarized light microscopy, transmission electron microscopy (TEM)

Received: April 23, 2025; Accepted: July 25, 2025

Skin Science Lab, School of Pharmacy, Kitasato University, 5-9-1, Shirokane, Minato-ku, Tokyo 108-8641, Japan DOI: 10.69336/acst.2025-05



© The Society of Cosmetic Chemists of Japan 2025

This article is licensed under a Creative Commons Attribution 4.0 International License.

^{*}Corresponding author: Katsunori Yoshida (E-mail: yoshida.katsunori@kitasato-u.ac.jp)

1. Introduction

Coacervation is a phenomenon in which 2 oppositely charged polyelectrolytes interact electrostatically in an aqueous solution, leading to liquid–liquid phase separation into a concentrated phase (coacervate) and a dilute phase. (and a dilute phase. A similar phenomenon occurs in surfactant micelles with oppositely charged polyelectrolytes. However, coacervation takes place only under specific conditions, and in many cases, mixtures of strongly charged polyelectrolytes and simple ionic surfactants undergo irreversible solid–liquid phase separation.

To better understand coacervation, studies have employed various model systems, such as modifying micelle surface charge density by mixing ionic surfactants with nonionic or amphoteric surfactants. Despite these efforts, many aspects of the mechanism remain unresolved. Previous research has demonstrated that coacervation results from the interplay of multiple factors. These include polymer properties (linear charge density, molecular weight, concentration, and molecular structure), micelle properties (surface charge density—defined by the ionic/amphoteric (nonionic) surfactant ratio—size, shape, and concentration), as well as temperature and ionic strength. 6-8,19-29)

In a system containing the cationic polymer, poly (diallyldimethylammonium chloride), the anionic surfactant, sodium dodecyl sulfate, and the nonionic surfactant Triton X-100, Wang et al. investigated the effects of polymer molecular weight, surfactant surface charge density, and the polymer/surfactant ratio.⁶⁾ The findings demonstrated that an increase in polymer molecular weight leads to a higher volume fraction of coacervate. Additionally, an increase in the surface charge density of surfactant micelles enhances electrostatic attraction between micelles and polymers, promoting complex formation. However, an excessive increase in micelle surface charge density strengthens electrostatic repulsion between micelles, that is, polymer–micelle complex, thereby suppressing coacervation. Furthermore, a 3-dimensional phase diagram was developed using polymer molecular weight, micelle surface charge density, and polymer/surfactant ratio as variables, systematically illustrating the influence of these factors on coacervation regions and physical properties. Wang et al.⁷⁾ also investigated the effect of salt concentration on coacervation, revealing that changes in salt concentration modulate the binding affinity between polymers and micelles, either promoting or inhibiting coacervation.

Due to its tunability, coacervate has been applied in various fields, including water treatment, DNA delivery to cells, and drug delivery.^{4,5,30–38)} One such application is shampoo formulation design. Shampoos typically contain cationic polymers as conditioning agents and anionic and amphoteric surfactants as detergents. Upon dilution with water during use, these components undergo coacervation, forming a coacervate that is insoluble in water. The properties of the coacervate, such as adhesion to hair and viscoelasticity, are known to significantly influence the sensory experience of the shampoos.^{4,5,25,39,40)}

Recently, driven by the Sustainable Development Goals and a growing preference for natural ingredients,⁴¹⁾ the use of amino acid-based surfactants—classified as non-sulfate surfactants—has been expanding in shampoo formulations. Compared to traditionally used lauryl ether sulfate (LES)- and lauryl sulfate (LS)-based shampoos, amino acid-based shampoos face challenges such as reduced foaming and thickening. However, due to their high biodegradability and low skin irritation, 42-44) they have become increasingly popular in the market. While extensive research has been conducted on the coacervation of LES/LS-based shampoos and their resulting coacervates, studies on coacervation in non-sulfate shampoos remain limited. As an initial investigation, we explored the correlation between coacervate properties and sensory attributes using commercial non-sulfate shampoos.⁴⁵⁾ Our findings confirmed that coacervation occurs in non-sulfate shampoos, just as in conventional sulfate shampoos, and that the physical properties of coacervates strongly influence the sensory experience of each product. Using a representative commercial non-sulfate shampoo, we examined coacervate formation and structural changes during the dilution process. 46) The results showed that the coacervates formed at higher dilution (lower relative concentration) were more elastic in nature, and at a relative concentration of around 0.05, the coacervates formed a lamellar liquid crystalline structure. Ilekti et al. previously investigated the structural evolution of coacervates in a mixture of the cationic surfactant, cetyltrimethylammonium bromide (CTABr), and the anionic polymer, sodium polyacrylate. 47,48) Their study revealed that a progressive ion-exchange process, in which Br⁻ (the counterion of CTABr) is replaced by PA⁻, alters micelle morphology and electrostatic interactions, ultimately affecting coacervate structure. Moreover, water content was found to play a critical role in this process. At low water content, micelles were densely packed into a hexagonal liquid crystalline phase, whereas at higher water content, micelle spacing increased, leading to the formation of a cubic liquid crystalline phase.

Previous studies on coacervates in commercial products faced challenges in examining the effects of polymer properties, micellar characteristics, and ionic strength on coacervation due to the unknown detailed composition of each ingredient. In this study, we developed a model shampoo with a well-defined composition, including

polymers, surfactants, and salt concentrations, to investigate coacervation and the physical properties of the resulting coacervates.

2. Materials and Methods

2.1. Materials

Cationized hydroxyethyl cellulose (nominal Mw 2.7×10^6 , $\alpha = 0.35$; Toho Chemical Industry, Tokyo, Japan) was used as the cationic polymer. For surfactants, sodium lauroyl aspartate (Asahi Kasei Finechem, Osaka, Japan) was used as an anionic surfactant, lauramidopropyl betaine (Kawaken Fine Chemicals, Tokyo, Japan) as an amphoteric surfactant, and cocamidomethyl monoethanolamine (Kao, Tokyo, Japan) as a nonionic surfactant. The chemical structures of the surfactants are shown in Fig. 1. Citric acid (Fuso Chemical Industry, Osaka, Japan) and sodium chloride (Naikai Salt Industry, Kurashiki, Japan) were used as purchased, and Milli-Q water was used as purified water.

The formulation of the model shampoo is shown in Table 1. The viscosity of the model shampoo after preparation was 0.64 Pa·s (Viscometer TV-25, rotor No. 3, 12 rpm, 25°C; Toki Sangyo, Tokyo, Japan), and the pH was 6.0, measured by a pH meter (F-72; HORIBA, Kyoto, Japan).

2.2. Turbidity measurement in shampoo dilution process

A fixed amount of shampoo solution was weighed and diluted with purified water under continuous stirring. The transmittance (%) of each diluted solution at 420 nm was measured using a U-2800 Spectrophotometer (Hitachi High-Tech, Tokyo, Japan). Turbidity was expressed as 100 – transmittance (%). The relative concentrations of diluted shampoo were calculated as follows:

Relative concentration = undiluted shampoo solution (g)/(undiluted shampoo solution (g) + added purified water (g)) Unless otherwise specified, all measurements, including turbidity assessments, were conducted at room temperature $(23^{\circ}C \pm 2^{\circ}C)$.

2.3. Coacervate formation

The shampoo and purified water were weighed in a 50-mL centrifuge vessel to achieve a relative concentration of 0.02–0.25. After mixing well, the mixture was centrifuged (4400 rpm \times 30 min) and left overnight. The supernatant was then removed, the weight w (g), including the container, was measured, and the weight of the coacervate produced was calculated by subtracting the previously measured empty weight w₀ (g) of the container from w (g). The weight of the coacervate obtained was divided by the weight of the shampoo used to calculate the amount of coacervate produced per 1 g of shampoo. Coacervate prepared by the same procedure was used to determine coacervate properties.

The concentration of solids in the coacervate (dry residual) was measured using the following procedure. A 0.1 g sample of the coacervate, prepared at each relative concentration, was weighed into a pre-weighed glass tube. The sample was then heated at 105°C for 2 hours. After heating, it was cooled in a desiccator with silica gel for 10 minutes at room temperature. The total weight, including the glass tube, was measured and the heating—cooling process was repeated until a constant weight was obtained. The dry weight of the coacervate was determined by subtracting the empty weight of the tube, and the percentage solids concentration was calculated accordingly.

2.4. Particle size and ζ -potential

The particle size and zeta (ζ)-potential of the coacervate were measured immediately after dilution using a dynamic light scattering instrument, ELSZ-1000 (Otsuka Electronics, Osaka, Japan). The ζ -potential was measured repeatedly 3 times at each relative concentration, and the average value was calculated. Particle size, diameter (d/nm), was determined using the Einstein–Stokes equation $D = kT/3\pi\eta d$, where D is the mutual diffusion coefficient obtained from dynamic light scattering. The average particle size and polydispersity index (PI) were calculated using the Cumulant method, as provided in the analysis software accompanying the measurement device.

2.5. Fluorescence probe measurement

A pyrene solution was prepared at a concentration of $0.5~\mu M$, and the sample solutions were then prepared using this solution to achieve a shampoo relative concentration range of 0.0001-0.1. Fluorescence spectra were measured using a fluorescence spectrophotometer (F-7000; Hitachi) with an excitation wavelength of 336 nm, a scanning range of 360-420 nm, an excitation slit width of 10 nm, and an emission slit width of 1 nm. The intensity ratio I_1/I_3 between the first and third fluorescence peaks was then calculated.

Fig. 1 Molecular structure. (A) Sodium lauroyl aspartate, (B) lauramidopropyl betaine, and (C) cocamide methyl monoethanolamine.

Table 1 Composition of a model shampoo.

•	*
Cationic hydroxyethyl cellulose	0.5% w/w
Sodium lauroyl aspartate	200 mM
Lauramidopropyl betaine	200 mM
Cocamide methyl monoethanolamine	105 mM
Citric acid	25 mM
Sodium chloride	200 mM
Water	q.s. (to 100%)

q.s., a sufficient quantity

2.6. Rheological measurement

Dynamic viscoelasticity measurements were conducted on the coacervates obtained at each relative concentration, as well as on the shampoo solution. A stress-controlled rheometer (Anton Paar MCR-300, with a 50-mm diameter parallel plate) was used for these measurements at 25°C, within a frequency range of $\omega = 0.1-100\,\text{rad/s}$. In the rheological measurements of the coacervate, strain sweep tests were conducted prior to frequency sweep measurements to identify the linear viscoelastic region, and the strain amplitude was set to 1%.

2.7. Polarized light microscopy

The coacervates produced at each relative concentration were observed with a polarized light microscope (OLYM-PUS BX51 equipped with sCMOS Microscope Camera Moticam S3; Shimadzu, Kyoto, Japan).

2.8. Transmission electron microscopy (TEM)

TEM observations were conducted at a relative concentration of 0.03 immediately after dilution. For TEM micrographs, 20 µL of diluted shampoo was placed on a 200-mesh size poly (vinyl formal)-coated copper grid and allowed to adsorb for 1 min. Excess liquid was removed with a piece of filter paper, air-dried, and then negatively stained with 2% aqueous uranyl acetate. The specimens were further dried *in vacuo* for 5 min before use. The specimens were examined under a transmission electron microscope (JEM-1400; JEOL, Tokyo, Japan) operating at an accelerating voltage of 120 kV at room temperature.

3. Results and Discussion

3.1. Turbidity measurement in shampoo dilution process

The results of turbidity measurements during the shampoo dilution process are shown in Fig. 2. The horizontal axis represents the relative concentration of shampoo diluted with water, while the vertical axis represents turbidity. At the right end of the horizontal axis, the relative concentration is 1 (undiluted shampoo solution), with increasing dilution toward the left. A value of 0.5 corresponds to a 2-fold dilution, and 0.1 corresponds to a 10-fold dilution. To better visualize changes in turbidity at low relative concentrations (high dilution), a logarithmic scale inset is included in Fig. 2. Throughout the dilution experiments, the pH remained around 6 for all relative concentrations, indicating that the carboxyl groups of the anionic surfactant were dissociated and carried a negative charge.

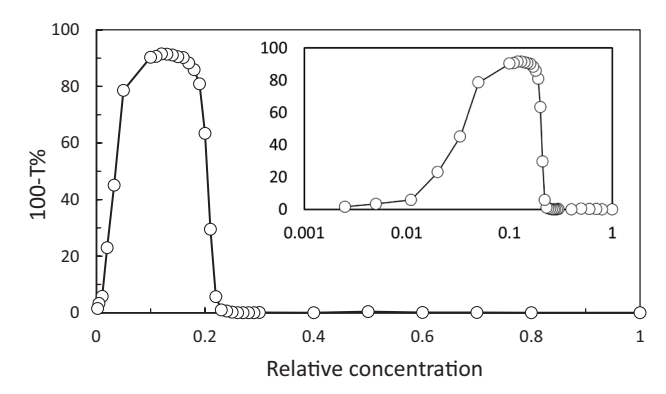


Fig. 2 Turbidity measurements of the diluted shampoo at various relative concentrations. The inset shows the same data plotted on a logarithmic scale. A relative concentration of 1 corresponds to the undiluted shampoo.

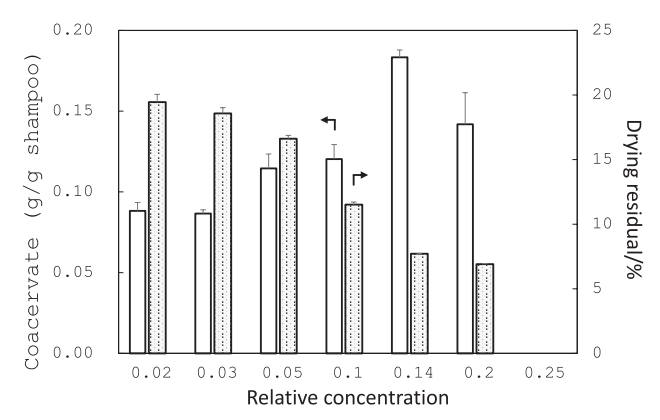


Fig. 3 Wet weight and drying residue of coacervate formed from the diluted shampoo at various relative concentrations. No measurable coacervate was collected at relative concentrations \geq 0.25 or <0.02. Left arrow: the left x-axis indicates the amount of coacervate. Right arrow: the right x-axis shows the drying residue of coacervate.

It is well known that the appearance of common shampoos changes from clear to cloudy and then back to transparent upon dilution. In this study, based on the premise that turbidity increases when coacervates form due to liquid–liquid phase separation, the coacervation region was defined as the range between the relative concentration at which turbidity begins to rise and the concentration at which it starts to decrease again.⁴⁾

In the model shampoo used in this study, an increase in turbidity was observed from a relative concentration of approximately 0.2, indicating coacervation, a liquid–liquid phase separation phenomenon. Upon further dilution with water, turbidity increased sharply, peaking at a relative concentration of around 0.1, and then gradually decreased at higher dilutions. This behavior—where turbidity rises rapidly at a certain relative concentration, remains elevated, and then gradually declines—is characteristic of coacervation and follows a typical bell-shaped curve.^{4, 6)}

3.2. Coacervate formation

Figure 3 shows the amount of coacervate formed at each relative concentration. The measurable coacervate first appeared at a relative concentration of 0.2, where turbidity began to abruptly increase and phase separation was initiated. At a relative concentration of 0.14, 0.18 g of coacervate per 1 g of shampoo was formed, and the amount of coacervate gradually decreased with further dilution. Below a relative concentration of 0.02, no measurable coacervate could be recovered by the present procedure.

As shown in Fig. 3, the dry residual of the coacervate was 6.9% at a relative concentration of 0.2, and it increased as dilution progressed, reaching 19.4% at a relative concentration of 0.02. These results indicate that as more water was added to the shampoo, a more concentrated coacervate with a higher solid content was obtained.

3.3. Particle size and ζ -potential

Figure 4 presents the results of turbidity, particle size, and ζ -potential measurements at each relative concentration. Particle size reached its maximum at a relative concentration of 0.1, coinciding with the peak in turbidity. The figure also includes the PI, showing that polydispersity increases as particle size increases. As dilution progresses and the relative concentration decreases, both particle size and PI decline in the region where turbidity decreases. Since turbidity is known

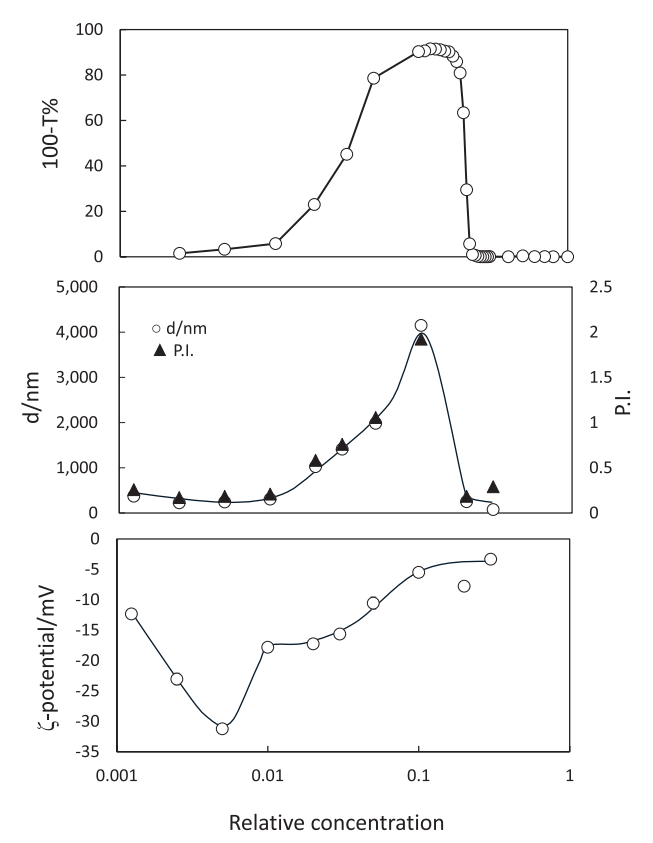


Fig. 4 Turbidity, DLS, and ζ-potential measurements of diluted shampoo at various relative concentrations. Lines in the figures are included as visual guides.

ζ, zeta; DLS, dynamic light scattering; PI, polydispersity index

to depend on both the concentration and volume of scattering particles, turbidity is thought to reflect the number and size of coacervate particles in this system. The experimental results for coacervate formation and particle size were generally consistent with the observed turbidity trends, supporting this interpretation. For example, in the case of Rayleigh scattering, the scattering intensity is proportional to the number of scatterers and to the cube of their volume (i.e., to the sixth power of the particle radius). Approximate values were estimated based on the amount of coacervate formed (Fig. 3) and the average particle size of the coacervate (Fig. 4). These estimations showed good agreement with the turbidity profiles presented in Fig. 2. However, because the coacervate particles are polydisperse, the measured particle sizes reflect transient values immediately after dilution, while phase separation continues over time. In addition, the refractive index contrast between the coacervate and the continuous phase may vary with relative concentration. As these calculations rely on several assumptions, a strictly quantitative discussion is challenging. Therefore, the detailed results of this analysis are not shown.

As shown in Fig. 4, below a relative concentration of 0.1, both the average particle size and PI decrease with further dilution, while the ζ -potential takes increasingly negative values (e.g., -5.5, -10.6, and -17.8 mV at relative concentrations of 0.1, 0.05, and 0.01, respectively). This suggests that the dispersion stability of the coacervate particles is enhanced at lower concentrations with electrostatic repulsive forces. Consequently, the absolute amount of coacervate formed also declines, making it difficult to measure coacervate formation at relative concentrations of 0.02 or lower, as the overall relative concentration of the system decreases.

The ζ -potential values across the relative concentration range in this experiment were negative at all measured points. At a relative concentration of 0.2, where coacervation begins, the ζ -potential was -7.7 mV. As dilution progressed, the negative charge increased, reaching a minimum of -31.2 mV at a relative concentration of 0.005. At even lower relative concentrations, the absolute value of the ζ -potential gradually decreased, approaching neutral and reaching -12.3 mV at the lowest measurable relative concentration of 0.00125. Previous studies on coacervation involving oppositely charged polyelectrolytes and surfactants have reported that coacervation occurs when the electrostatic repulsion within the polyelectrolyte–surfactant complex decreases near electroneutrality, making the complex more prone to aggregation. (48,49) In our system, we initially expected the ζ -potential to be around ± 0 mV at a relative concentration of 0.1, where turbidity

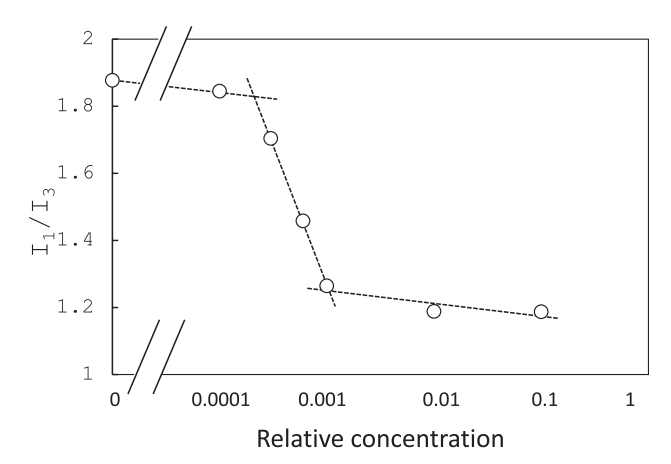


Fig. 5 I_1/I_3 intensity ratio for pyrene (0.5 μ M) fluorescence in diluted shampoo as a function of relative concentration. Lines in the figure are included as visual guides.

was highest and the average particle size was largest. However, as shown in Fig. 4, the actual results differed significantly from this expectation. The reasons for this discrepancy are discussed later in this article.

3.4. Fluorescent probe measurement

To investigate the surfactant aggregation state in the diluted region observed in the ζ -potential measurements, fluorescence measurements were performed using pyrene as a probe. The fluorescence spectrum of pyrene is known to change depending on its surrounding hydrophilic/hydrophobic environment.^{50–52)} By looking at the ratio of the first peak of pyrene fluorescence around 374 nm (I_1) to the third peak around 385 nm (I_3) (I_1/I_3), the environment in which pyrene is present can be estimated, and the critical micelle concentration of surfactants and critical aggregation concentration (CAC) in the presence of polymer have been measured using this property.⁵³⁾

As shown in Fig. 5, the results present a typical curve with 2 inflection points, occurring around relative concentrations of 0.001 and 0.0002. In the relative concentration range above 0.001, there exists a sufficiently hydrophobic micellar core to solubilize most of the pyrene molecules in the system. However, at lower relative concentrations, the micelle concentration capable of solubilizing pyrene gradually decreases with dilution, and below a relative concentration of 0.0002, surfactant micelles are dissociated, leaving only monodisperse surfactant molecules dissolved in the system, where pyrene molecules are dissolved in water.

Estimating the CAC based on the midpoint between the 2 bending points, this midpoint suggests a CAC around a relative concentration of 0.0004. Considering that the model shampoo contains 200 mM anionic surfactants, 0.08 mM is comparable to the previously reported CAC of 0.04 mM for systems involving cationic cellulose and LS.^{53,54)}

Considering the ζ -potential trends discussed earlier and fluorescence probe analysis results, it is suggested that negatively charged complexes are formed between the cationic polymers and the mixed micelles of anionic and amphoteric surfactants with the dilution of the shampoo up to a relative concentration of 0.001. In this region, a sufficient number of micelles are formed solubilizing the fluorescent probe pyrene. The average molecular weight per cationic group unit of the polymer, calculated from the structure of cationic hydroxyethyl cellulose (α = 0.35) used in this experiment, is 326. This corresponds to a cationic group molar concentration of 15.3 mM in the shampoo with 0.5% polymer. Meanwhile, the anionic surfactant concentration in the model shampoo is 200 mM, indicating that the system has an overall excess of negative charge. Compared with the previous study by Wang et al.,^{6,7)} which investigated systems composed of equal charge molar ratios of cations and anions, our system consisting of excess anions may cause the formation of negatively charged complexes. We are currently investigating coacervation with a variety of polymer/surfactant ratios, including equimolar cation and anion systems. The results will be reported accordingly.

In entropy-driven coacervation with counterion release, as the system is diluted with water, counterions (Na⁺ and Cl⁻ in this case) are released into the dilute phase, strengthening the electrostatic interactions between the cationic polymer and anionic surfactant.^{55–58)} Consequently, the number of anionic surfactant molecules bound per polymer (i.e., the number of micelles) increases. In the system with excess anionic surfactant, as shown in Fig. 4, the ζ -potential becomes more negative with dilution in the relative concentration range of 0.3–0.005. With further dilution, at relative concentrations below 0.001, the system approaches the CAC, and the surfactants gradually lose their ability to form

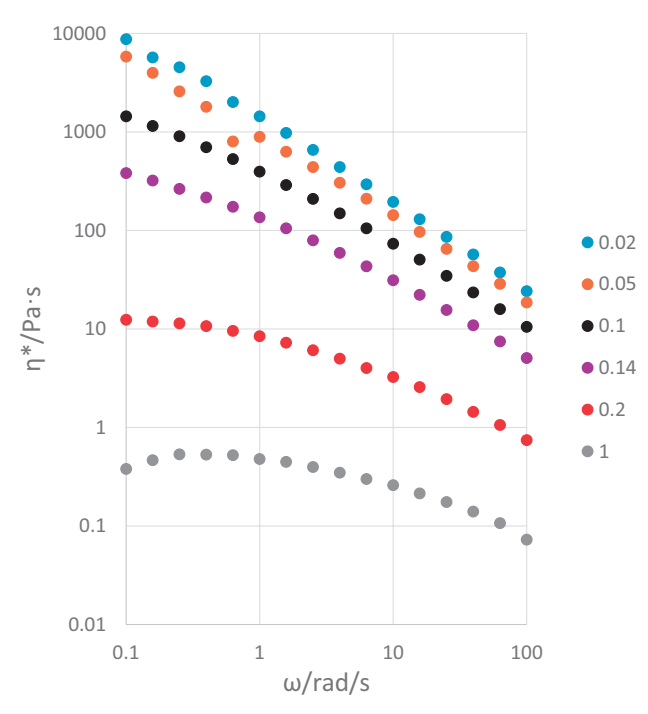


Fig. 6 Complex viscosity (η^*) of the shampoo and coacervate formed at various relative concentrations. The relative concentrations are indicated in the figure. Coacervate samples were prepared following the same procedure as described for the coacervate weight measurements in Fig. 2.

micelles. As a result, monodisperse dissolved surfactants become dominant in the system. The anionic surfactant desorbs from the cationic polymer, and the ζ -potential of the complex shifts toward neutrality. It is presumed that the electrical neutralization point occurs between the first and second bending points of pyrene I_1/I_3 (relative concentration 0.0002–0.001), where the ζ -potential may approach 0 mV. However, in this study, the exact relative concentration at which electrical neutralization occurs could not be determined, as it fell below the measurement limit of the instrument in such a diluted region.

3.5. Rheological measurement

Figures 6 and 7 show the results of dynamic viscoelasticity measurements of the shampoo solution and coacervate. In general, the viscosity of shampoos is increased by adding salt, which is promoted by the growth of mixed mixelles composed of anionic and amphoteric surfactants, stimulating the growth of mixelles into elongated ones. The η^* values of the coacervates show that coacervates obtained at higher dilution, corresponding to lower relative concentrations, exhibit higher viscosity, suggesting the formation of more structured viscous networks.

Figure 7 shows the frequency dependence of the storage modulus G' and loss modulus G'' obtained under the same measurement conditions. In the undiluted shampoo solution, G' < G'' over the entire measured frequency range, indicating that the viscous component dominates. However, for coacervates at relative concentrations between 0.1 and 0.2, G' and G'' intersect, with the intersection point shifting toward lower frequencies implying longer relaxation times as the relative concentration decreases. For coacervates at relative concentrations below 0.05, G' > G'' across all measured frequencies, signifying the formation of a gel-like structure. Although the gel-like viscoelastic properties of coacervates have been reported for conventional sulfate-based shampoos,⁴⁾ the pronounced change in flow behavior with dilution concentration appears to be a characteristic feature of our formula.

Green and Tobolsky predicted that the high-frequency storage modulus G_H follows the relation $G_H = vkT$, where v is the number density of elastically effective chains, k is Boltzmann's constant, and T is the absolute temperature. In this study, the G' value at 100 rad/s for the coacervates obtained at each relative concentration was used as G_H and plotted against relative concentration, as shown in Fig. 8. Ilekti et al. reported that in the CTABr/PANa system, dilution leads to the release of counterions from the coacervate phase into the dilute phase, 47,48 resulting in an increased solids concentration in the coacervate phase (i.e., the polymer-rich phase). Our results of drying residual of coacervates shown in Fig. 2 are in good agreement with this finding. At lower relative concentrations, electrostatic cross-linking between the trimethylammonium groups of the cationic polymer and the carboxyl groups of the anionic surfactant increases as Na^+ and Cl^- ions are expelled

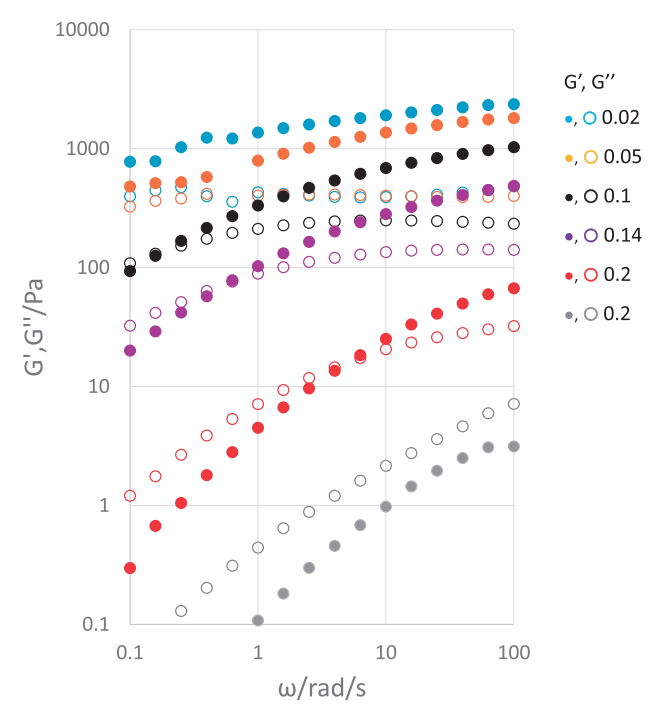


Fig. 7 Storage modulus (G') and loss modulus (G") of the shampoo and coacervate formed at various relative concentrations. The relative concentrations are indicated in the figure. Coacervate samples were prepared following the same procedure as described for the coacervate weight measurements in Fig. 2.

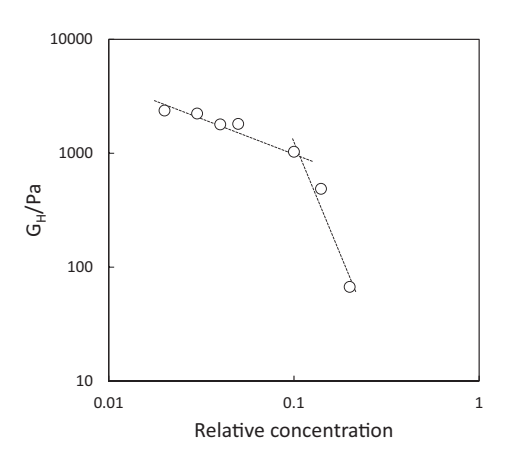


Fig. 8 High-frequency storage modulus (G_H) of the coacervate formed from diluted shampoo at various relative concentrations. The G_H values represent G' at 100 rad/s. Lines in the figure are included as visual guides.

into the dilute phase, leading to enhanced elasticity in the system. In Fig. 8, a bending point is observed at a relative concentration of 0.1, suggesting that a structural transition of coacervate occurs around this concentration.

3.6. Polarized light microscopy

Figure 9 shows the results of polarized light microscopy of coacervates obtained at relative concentrations around 0.1, where structural changes are expected based on the viscoelasticity measurements. At relative concentrations of 0.14 and 0.1, a texture characteristic of the hexagonal liquid crystalline structure was observed. As the relative concentration decreased, larger structures with higher brightness appeared. In contrast, at relative concentrations of 0.05 and 0.02, a texture characteristic of the lamellar liquid crystalline phase, known as "oily streaks," was observed. This indicates a structural transition in the coacervate from a hexagonal to a lamellar phase around a relative concentration of 0.1. This finding is in good agreement with the change in G_H shown in Fig. 8.

3.7. TEM

Figure 10 displays TEM images of the coacervate at a relative concentration of 0.03. The images represent the coacervate dispersion immediately after dilution, as the coacervate itself, with its high viscosity as previously analyzed, was

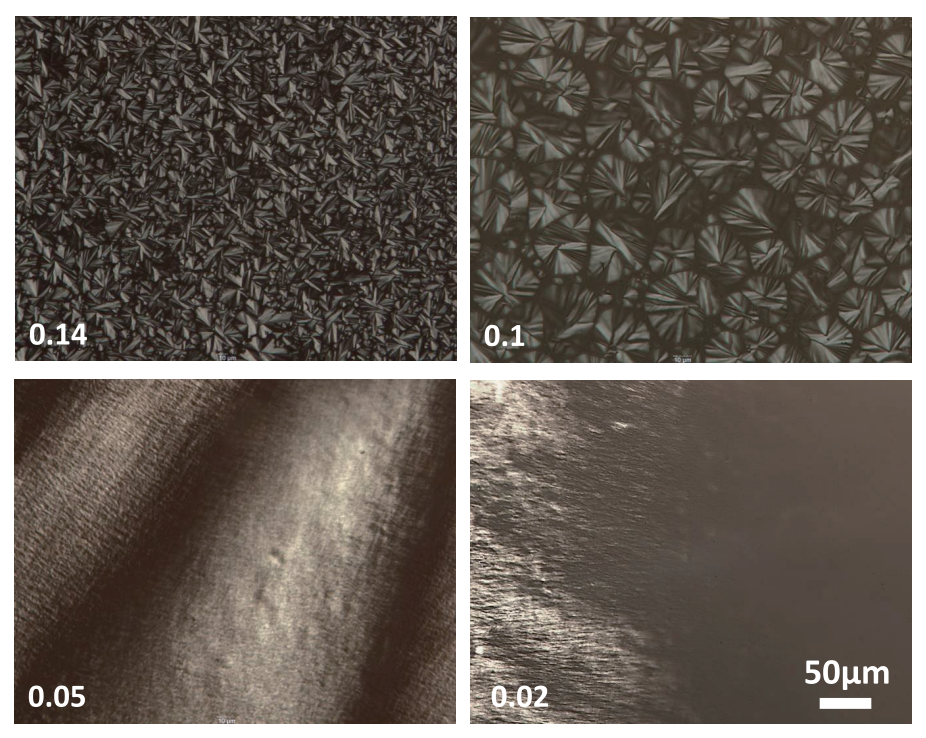


Fig. 9 Polarized light microscopic images of the coacervate formed from diluted shampoo at relative concentrations of 0.02, 0.05, 0.1, and 0.14. The coacervate samples were prepared following the same procedure used for coacervate amount measurements in Fig. 2. All images shown were taken at the same magnification.

too thick for thinning for the TEM observation. The TEM image also reveals that the dispersed coacervate particles are enveloped by a distinct multilayered structure.

3.8. Model of coacervate structural change with dilution

Based on the observations made thus far in our model shampoo system, a model diagram illustrating the coacervation phenomenon and the structural changes associated with dilution is presented in Fig. 11. As dilution proceeds from the right side of the figure, the system initially consists of positively charged cationic polymers and negatively charged anionic/amphoteric surfactant mixed micelles in the shampoo solution (I). At a relative concentration of approximately 0.3, before phase separation occurs, the anionic/amphoteric surfactants exist as spherical micelles. However, as the relative concentration decreases to around 0.2, where phase separation begins, the adsorption of cationic polymers onto the micelle surfaces increases. Beyond this critical relative concentration, phase separation takes place, forming a coacervate phase composed of the surfactant-polymer complex and a dilute phase containing primarily water, surfactants, and counterions (II). During the initial phase separation, the coacervate forms a hexagonal liquid crystalline structure, which transitions to a lamellar liquid crystalline structure at relative concentrations below 0.1. According to the findings of Ilekti et al., 47,48) the driving force for coacervation is the increase in entropy due to counterion release. As dilution progresses, the small counterion of anionic surfactant undergoes ion exchange to the cationic polymer, which may lead to a structural transformation of the surfactant molecular assembly, characterized by changes in interfacial curvature^{61,62)} as more cationic polymer cooperatively binds to the micelle surface. This reduces the electrostatic repulsion between the hydrophilic groups of the anionic surfactant, leading to an increase in critical packing parameter and the formation of hexagonal and lamellar crystalline structures.

With dilution, the viscosity and elasticity of the coacervate increase as electrostatic cross-linking points between the polymers and micelles increase, forming a network. With further dilution, the binding between the polymer and surfactant micelles strengthens, increasing the number of negatively charged micelles (anionic/amphoteric surfactants) bound per polymer. As a result, the negative charge of the complex increases (ζ -potential decreases), leading to redispersion of the polymer–surfactant complex (III). With further dilution below CAC, the micelles dissociate, with some anionic surfactants adsorbed onto the cationic polymer, while most of the surfactants exist in a monodisperse dissolved state (IV).

In this study, we investigated coacervation during the dilution process and the structure of the coacervate formed in a model non-sulfate shampoo with sodium lauroyl aspartate and lauramidopropyl betaine. Consistent with our

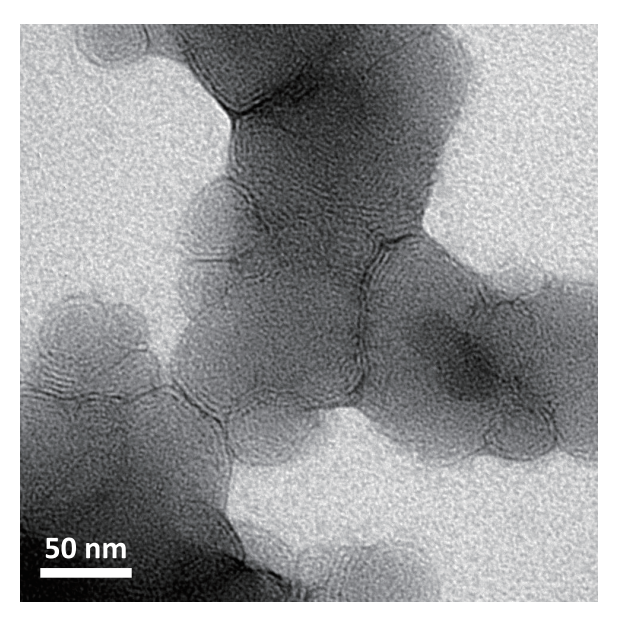


Fig. 10 TEM observation of the coacervate at a relative concentration of 0.03. The sample was analyzed immediately after dilution.

TEM, transmission electron microscopy

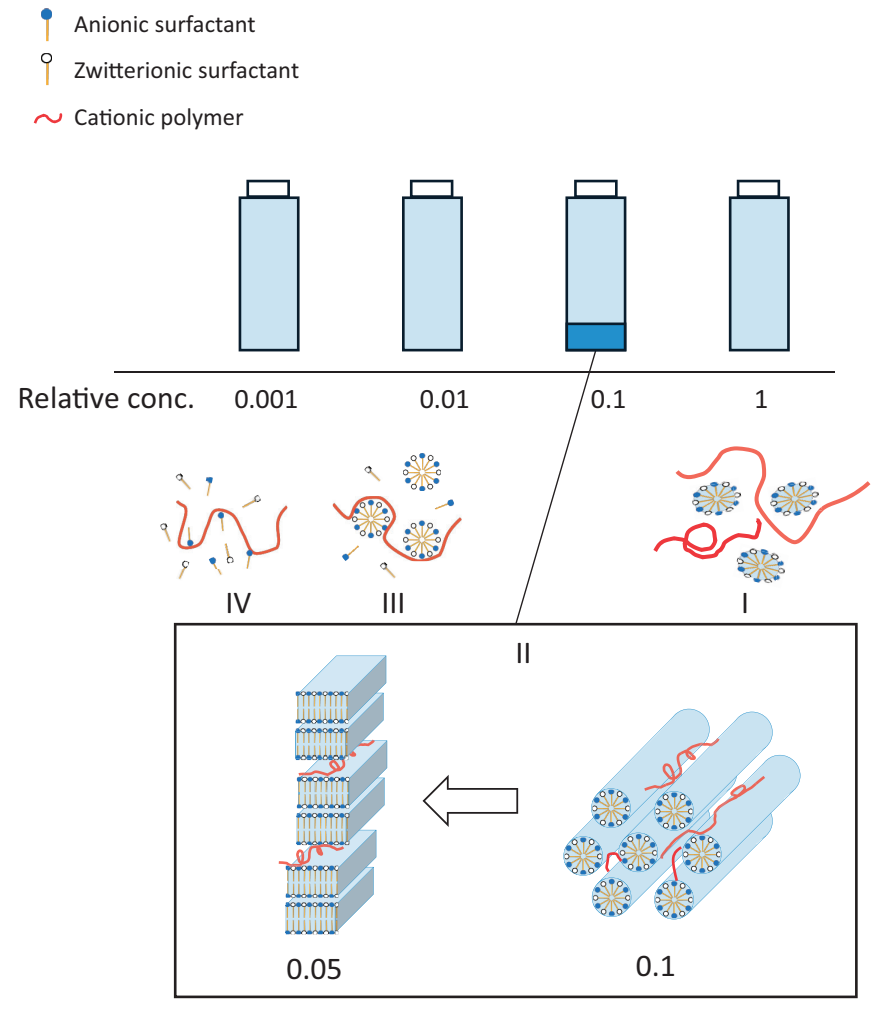


Fig. 11 Schematic illustration of coacervate structural transition through dilution. The figure is a conceptual diagram in which the sizes and molecular numbers of the polymers and surfactants are disregarded.

previous studies on commercial non-sulfate shampoos,⁴⁶⁾ the coacervate in our model formula was also found to form a lamellar structure at a certain relative concentration. However, in the present model shampoo, the coacervate initially exhibited a hexagonal structure before transitioning to a lamellar one. Notably, to the best of the authors' knowledge, reports of coacervates forming a specific structure and subsequently undergoing a structural transition are scarce among any surfactant systems including conventional sulfate shampoos, making this an interesting observation.

For this model shampoo, the cationic polymers and surfactants were selected based on one of the previously mentioned commercial non-sulfate shampoos. We are currently investigating whether the formation of hexagonal and lamellar structures is specific to the combination and concentration of the cationic polymer and surfactant used in this study by varying the ratio and type of anionic surfactants. As a future prospect, we aim to further refine the model formula by adjusting the molecular weight and degree of cationization of the cationic polymers to elucidate their effects on coacervation.

4. Conclusion

The dilution of shampoo with water during use induces electrostatic interactions among the cationic polymer, anionic surfactants, and amphoteric surfactants, leading to the formation of coacervates. In this study, we focused on the coacervation process and the structural changes of the coacervate formed in a model formulation of a non-sulfate shampoo with sodium lauroyl aspartate and lauramidopropyl betaine. Our findings indicate that the coacervate is more concentrated with dilution. Furthermore, the initially formed coacervate, which forms a hexagonal liquid crystalline structure upon phase separation, transitions to a lamellar structure at a relative concentration of approximately 0.1. With further dilution, the lamellar structure gradually disappears, leading to the dissolution of the coacervate. To gain a deeper understanding of these structural changes, further investigations are needed to determine whether similar transitions occur in other systems by varying the type and composition of surfactants, polymer molecular weight, degree of cationic modification, and other relevant factors.

Acknowledgments: The authors thank Toho Chemical Industry for their kind gift of cationized hydroxyethyl cellulose. A part of this work was supported by Advanced Research Infrastructure for Materials and Nanotechnology in Japan (ARIM) of the Ministry of Education, Culture, Sports, Science and Technology (MEXT) (Grant Number JPMXP1224UT).

Conflict of Interest: None.

Abbreviations: CAC, critical aggregation concentration; CTABr, cetyltrimethylammonium bromide; LES, lauryl ether sulfate; LS, lauryl sulfate; PI, polydispersity index; TEM, transmission electron microscopy

References

- 1) J. Van der Gucht, E. Spruijt, M. Lemmers, M.A.C. Stuart, J. Colloid Interface Sci., 361, 407–422 (2011)
- 2) J. Yuan, H. Tanaka, Nat. Commun., 16, 1517 (2025)
- 3) P.L. Dubin, M. Elayne, Y. Vea, M.A. Fallon, S.S. Thé, D.R. Rigsbee, L.M. Gan, Langmuir, 6, 1422–1427 (1990)
- 4) Y. Hiwatari, K. Yoshida, T. Akutsu, M. Yabu, S. Iwai, J. Soc. Cosmet. Chem. Jpn., 38, 211–219 (2004)
- 5) Y. Yamamoto, T. Ono, J. Soc. Cosmet. Chem. Jpn., 57, 50–57 (2023)
- 6) Y. Wang, K. Kimura, P.L. Dubin, W. Jaeger, Macromolecules, 33, 3324–3331 (2000)
- 7) Y. Wang, K. Kimura, Q. Huang, P.L. Dubin, W. Jaeger, Macromolecules, 32, 7128-7134 (1999)
- 8) E. Kizilay, A.B. Kayitmazer, P.L. Dubin, Adv. Colloid Interface Sci., 167, 24–37 (2011)
- 9) C. Seyrig, G. Kignelman, W. Thielemans, P.L. Griel, N. Cowieson, J. Perez, N. Baccile, Langmuir, 36, 8839–8857 (2020)
- 10) N. Kanei, T. Kodama, T. Harigai, J. Soc. Cosmet. Chem. Jpn., 51, 311–316 (2017)
- 11) E.D. Goddard, R.B. Hannan, J. Am. Oil Chem. Soc., 54, 561–566 (1977)
- 12) Q. Wang, J.B. Schlenoff, Macromolecules, 47, 3108–3116 (2014)
- 13) K. Ohbu, O. Hiraishi, I. Kashiwa, J. Am. Oil Chem. Soc., 59, 108–112 (1982)
- 14) K. Thalberg, B. Lindman, K. Bergfeld, Langmuir, 7, 2893–2898 (1991)
- 15) K. Thalberg, B. Lindman, G. Karlstrom, J. Phys. Chem., 94, 4289–4295 (1990)

- 16) K. Thalberg, B. Lindman, G. Karlstrom, J. Phys. Chem., 95, 3370–3376 (1991)
- 17) K. Thalberg, B. Lindman, G. Karlstrom, J. Phys. Chem., 95, 6004–6011 (1991)
- 18) A. Hashidzume, K. Yoshida, Y. Morishima, P.L. Dubin, J. Phys. Chem. A, 106, 2007–2013 (2002)
- 19) K. Yoshida, Y. Morishima, P.L. Dubin, M. Mizusaki, Macromolecules, 30, 6208–6214 (1997)
- 20) K. Yoshida, S. Sokhakian, P.L. Dubin, J. Colloid Interface Sci., 205, 257–264 (1998)
- 21) P.L. Dubin, R. Oteri, J. Colloid Interface Sci., 95, 453–461 (1983)
- 22) P.L. Dubin, M.E. Curran, J. Hua, Langmuir, 6, 707–709 (1990)
- 23) D.W. McQuigg, J.I. Kaplan, P.L. Dubin, J. Phys. Chem., 96, 1973–1978 (1992)
- 24) L. Piculell, B. Lindman, Adv. Colloid Interface Sci., 41, 149–178 (1992)
- 25) M. Miyake, Adv. Colloid Interface Sci., 239, 146–157 (2017)
- 26) A.Y. Xu, E. Kizilay, S. P. Madro, J. Z. Vadenais, K. W. McDonald, P.L. Dubin, Soft Matter, 14, 2391–2399 (2018)
- 27) Y. Morishima, M. Mizusaki, K. Yoshida, P.L. Dubin, Colloids Surf. A Physicochem. Eng. Asp., 147, 149–159 (1999)
- 28) K. Yoshida, P.L. Dubin, Colloids Surf. A Physicochem. Eng. Asp., 147, 161–167 (1999)
- 29) A.B. Kayitmazer, Adv. Colloid Interface Sci., 239, 169–177 (2017)
- 30) M. Ghasemi, S.N. Jamadagni, E. S. Johnson, R. G. Larson, Langmuir, 39, 10335–10351 (2023)
- 31) C. Schmitt, S.L. Turgeon, Adv. Colloid Interface Sci., 167, 63–70 (2011)
- 32) B.D. Winslow, H. Shao, R.J. Stewart, P. A. Tresco, Biomaterials, 31, 9373-9381 (2010)
- 33) N.R. Johnson, Y. Wang, Expert Opin. Drug Deliv., 11, 1829–1832 (2014)
- 34) L. Chiappisi, M. Simon, M. Gradzielski, ACS Appl. Mater. Interfaces, 7, 6139–6145 (2015)
- 35) D.J. Burgess, S. Ponsart, J. Microencapsul., 15, 569–579 (1998)
- 36) Y. Wang, J. Gao, P.L. Dubin, Biotechnol. Prog., 12, 356–362 (1996)
- 37) O.G. Jones, U. Lesmes, P.L. Dubin, D.J. McClements, Food Hydrocoll., 24, 374–383 (2010)
- 38) M. Mizusaki, Y. Morishima, K. Yoshida, P. L. Dubin, Langmuir, 13, 6941–6946 (1997)
- 39) M. Sakaguchi, E. Suenaga, K. Kawaguchi, J. Soc. Cosmet. Chem. Jpn., 53, 106–111 (2019)
- 40) M. Ezure, J. Jpn. Cosmet. Sci. Soc., 42, 15-20 (2018)
- 41) Y. Koizumi, Fragrance Journal, 50, 10–16 (2022)
- 42) Y. Hoshino, Y. Tsuchimochi, N. Sekiguchi, J. Soc. Cosmet. Chem. Jpn., 53, 207–214 (2019)
- 43) E. Shiojiri, K. Sano, M. Koyama, M. Ino, T. Hattori, H. Yoshihara, K. Iwasaki, Y. Kawasaki, J. Soc. Cosmet. Chem. Jpn., 30, 410–418 (1996)
- 44) K. Sakamoto, J. Oleo Sci., 44, 18–27 (1995)
- 45) H. Kamo, T. Mori, K. Yoshida, J. Soc. Cosmet. Chem. Jpn., 59, 88–94 (2025)
- 46) H. Kamo, T. Mori, K. Yoshida, Appl. Cosmetic Sci. & Tech., Accepted for publication
- 47) P. Ilekti, L. Piculell, F. Tournilhac, B. Cabane, J. Phys. Chem. B, 102, 344–351 (1998)
- 48) P. Ilekti, T. Martin, B. Cabane, L. Piculell, J. Phys. Chem. B, 103, 9831–9840 (1999)
- 49) E. Kizilay, A. B. Kayitmazer, P.L. Duin, Adv. Colloid Interface Sci., 167, 24–37 (2011)
- 50) M.E. Haque, S. Ray, A. Charkrabarti, J. Fluoresc., 10, 1–6 (2000)
- 51) D.C. Dong, M. A. Winnik, Photochem. Photobiol., 35, 17–21 (1982)
- 52) G.B. Ray, I. Chakraborty, S.P. Moulik, J. Colloid Interface Sci., 294, 248–254 (2006)
- 53) J. Lee, Y. Moroi, Langmuir, 20, 4376–4379 (2004)
- 54) T. Iwasaki, M. Ogawa, K. Esumi, K. Meguro, Langmuir, 7, 30–35 (1991)
- 55) J. Gummel, F. Cousin, F. Boue, J. Am. Chem. Soc., 129, 5806–5807 (2007)
- 56) Z. Ou, M. Muthukumar, J. Chem. Phys., 124, 15492 (2006)
- 57) S. Park, R. Barnes, Y. Lin, B. Jeon, S. Najafi, K.T. Delaney, G.H. Fredrickson, J.E. Shea, D.S. Hwang, S. Han, Commun. Chem., 3, 83 (2020)
- 58) M. Ghasemi, S. Friedowitz, R.G. Larson, Soft Matter, 16, 10640–10656 (2020)
- 59) M.S. Green, A.V. Tobolsky, J. Chem. Phys., 14, 80–89 (1946)
- 60) T. Annable, R. Buscall, R. Ettelaie, D. Whittlestone, J. Rheol. (N.Y.N.Y.), 37, 695–726 (1993)
- 61) K. Aramaki, Oleoscience, 23, 37–41 (2023)
- 62) K. Aramaki, J. Jpn. Soc. Colour Mater, 89, 98–101 (2016)